Biotribology 30 (2022) 100210

Contents lists available at ScienceDirect

Biotribology

journal homepage: www.elsevier.com/locate/biotri

Frictional Properties of a Novel Artificial Snakeskin for Soft Robotics

Frederik Lamping [a,*], Stanislav N. Gorb [b], Kristin M. de Payrebrune [a]

[a] Institute for Computational Physics in Engineering, TU Kaiserslautern, Erwin-Schroedinger-Str. 56, 67663 Kaiserslautern, Germany
[b] Department Functional Morphology and Biomechanics, University of Kiel, Am Botanischen Garten 1-9, 24118 Kiel, Germany

ARTICLE INFO

Keywords:
Artificial snakeskin
Soft robotics
Snake-like robots
Friction anisotropy
Modular design

ABSTRACT

Although snake-like robots are only rarely used in real applications, numerous designs have been proposed by different researchers. In addition to the capability of grasping objects by bending their body around them, snakes travel in various environments by using different gaits. To move forward, they need a skin which provides friction anisotropy to the ground. The designs of snake-like robots vary in their actuation mechanism as well as in the design of their artificial skin. In this work, we present a novel design of an artificial snakeskin. The design is related to an application in soft robotics, but is not restricted to this type of robot. Since soft robots are flexible and can stretch, our artificial skin is also able to. It is inspired by the belly of snakes and provides friction anisotropy in forward-reverse direction. To achieve this, we embed scales with a specific angle of attack into a flexible base body. In the experimental investigation of the artificial snakeskin, we determine the friction anisotropy for two base body materials with different stiffness and for three angles of attack. Although the development of the artificial skin is at an early stage, the results of the experimental investigation are promising. The dynamic behavior of the artificial snakeskin indicates that a flexible base material reduces friction in forward direction and increases friction in reverse direction, thus enhancing friction anisotropy. Furthermore, the results obtained give important information for further design improvements in future.

Presentation of a modular and stretchable artificial snakeskin Systematic investigation of the frictional properties when changing the angle of attack of the scales and the softness of the base material the scales are embedded in A soft base material increases friction anisotropy and reduces inaccuracies of hand manufacturing Demonstration of a soft robotic actuator which uses the artificial snakeskin for crawling.

1. Introduction

Although limbless, the locomotion of snakes is versatile. Besides four common gaits when moving on the ground [1], snakes are capable to swim, to climb trees, and to grasp objects. This versatility might be a reason why the investigation of the locomotion of snakes has attracted researchers in the past, like Shigeo Hirose in 1976 [2], and continues to do so today. Recent research addresses several aspects of the snakes' locomotion, like the biomechanics [3,4], the friction anisotropy [5,6], the motion of the scales [7], and their surface microstructure [8]. A comprehensive summary of the latest findings is given in [1].

Not only the investigation of snakes is of interest to researchers, but also the bio-inspired design of snake-like robots. Although snake-like robots are not common in everyday use, new designs are continuously being developed. A review of older designs is given in [9], while [10] enlightens the state of the art of the modeling of snake-like robots.

In order to generate propulsion, friction anisotropy between the snake-like robot and the ground is crucial. There are different approaches of how to achieve friction anisotropy, using fixed stiff scales [11], movable stiff scales [12], a 3D-printed surface with scales [13], or wheels [14].

Soft robotics are an interesting new field of robotics. Instead of stiff materials and joints, these robots consist of flexible materials and allow deformations, which have not been possible before. A review on the newest designs of soft robots is given in [15]. Although most of the previously mentioned snake-like robots are made of stiff materials, there is some effort to develop snake-like soft robots as well [14,16–18].

In soft robotics, an artificial snakeskin needs to be stretchable in order to deform together with the robot and to follow its motion. From a designer's perspective, there are two possibilities to achieve this: either the artificial skin consists of numerous small elements, which are fixed separately to the body of the robot, or the skin itself is flexible.

Ta et al. [18] present an approach which uses a multitude of flexible elements to achieve friction anisotropy for a snake-like soft robot. The

* Corresponding author.
E-mail addresses: frederik.lamping@mv.uni-kl.de (F. Lamping), sgorb@zoologie.uni-kiel.de (S.N. Gorb), kristin.payrebrune@mv.uni-kl.de (K.M. de Payrebrune).

https://doi.org/10.1016/j.biotri.2022.100210
Received 31 July 2021; Received in revised form 22 March 2022; Accepted 28 April 2022
Available online 4 May 2022
2352-5738/© 2022 Elsevier Ltd. All rights reserved.

flexible elements bend depending on the direction of locomotion such that they touch the ground with direction-depending areas. By using areas with different coefficients of friction, friction anisotropy can be achieved. This working principle is interesting for surfaces with a relatively low roughness, but will probably fail in an outdoor-application.

A famous approach of an artificial skin for soft robots is the so-called kirigami skin of Rafsanjani et al. [17]. It is based on a polyester sheet with an incised pattern, which is wrapped around the robot. When the robot stretches the polyester sheet stretches as well and the scales lift from the body. The original design focuses on rectilinear locomotion, while improved designs are applied to an earthworm-like robot [19], and with a focus on transverse friction [20]. However, the angle of attack of the scales of the kirigami skin is kinematically connected to the stretch of the robot, which prevents to tune this important parameter.

In this work, we present a novel approach of an artificial snakeskin for snake-like soft robots. Due to its modularity, it is advantageous for a systematical investigation of the influence of single parameters on the frictional properties. In the following, we will first introduce the design of the artificial skin in Section 2. Hereby, we refer to the works of other researchers which gave inspiration for our design. In Section 3, we describe the experimental setup to determine the frictional properties of the artificial snakeskin. In Section 4, we analyze the test data and, finally, conclude our findings in Section 5.

2. Design

The artificial skin is intended to be mounted on a universal soft bending actuator as shown in Fig. 1a [21]. The actuator consists of three fiber-reinforced silicone cylinders in parallel alignment. The fiber reinforcement causes the cylinders to stretch when pressurized, which leads to a continuous bending if one cylinder is longer than the others, and/or to a stretching if multiple cylinders are elongated simultaneously. Several bending actuators connected in series represent a snake-like soft robot being able to bend and to stretch. The artificial snakeskin is supposed to be mounted on the bottom of the bending actuator as shown in Fig. 1b.

2.1. Inspiration

With respect to already published simulations, prototypes and test results, we identified the following aspects as the most relevant to develop an artificial snakeskin with high friction anisotropy:

1. stiffness of mounting at the base [5,7],
2. angle of attack of the scales,
3. shape of the scale's edges [7],
4. microstructure of the scales' surface [8].

This study focuses on the first two aspects to find a beneficial basic design by a systematical investigation, while the third and forth aspect are related to the surface of the scales and are left to future work.

Marvi et al. [7] derived a numerical model which gives evidence that snakes actively actuate their scales. By applying a moment to the scales, the friction of the snakeskin increases in reverse direction because the scales are forced to interlock with surface irregularities. This result is in agreement with a study of Filippov and Gorb [5], who numerically investigated the friction anisotropy of a stiff scale embedded in a soft material and sliding over a non-smooth surface. The model approximates a biological mechanism that provides friction anisotropy and is used by multiple animals, including snakes. In contrast to Marvi et al. [7], the model assumes elastic forces of the soft material acting on the scales instead of an active actuation. One of the key-findings of Filippov and Gorb [5] is that the highest friction anisotropy occurs for an intermediate stiffness of the embedding material. The imitation of this phenomenon is a promising approach for artificial snakeskin. Note that "intermediate" is a relative specification since the total stiffness depends on the other parameters of the system, i.e. the load applied and the length of the scales.

The necessity of finding a beneficial angle of attack is the consequence of these thoughts. When the scales are embedded in a flexible material and are not actively actuated, the preadjusted angle of attack has a significant influence on the smallest and the largest dynamic angle and thus on the friction anisotropy.

2.2. Design

Based on the findings mentioned in Subsection 2.1, our aim is to analyze single parameters of a snakeskin individually. Due to its modularity, our artificial snakeskin is designated for a systematic investigation of the stiffness of mounting of the scales, and their angle of attack. The design is inspired by the belly scales of real snakes. As shown in Fig. 1c, the artificial snakeskin consists of three components: a base body for a flexible mounting of the scales, brackets to define a desired angle of attack and to fix the scales, and the scales themselves. The use of flexible base material embedding the brackets originates from the patent of a non-stretchable artificial snakeskin [22]. The components will be described in the following.

2.2.1. Base Body

The base body keeps the brackets in position and fulfills two tasks. On the one hand, it provides a flexible mounting of the scales, which increases the friction anisotropy of the artificial skin when a beneficial stiffness is chosen. On the other hand, a flexible base body material provides the possibility to mount the artificial snakeskin on a soft robot with only little effect on its motion.

Silicone rubber is widely used for soft robotics and there are many

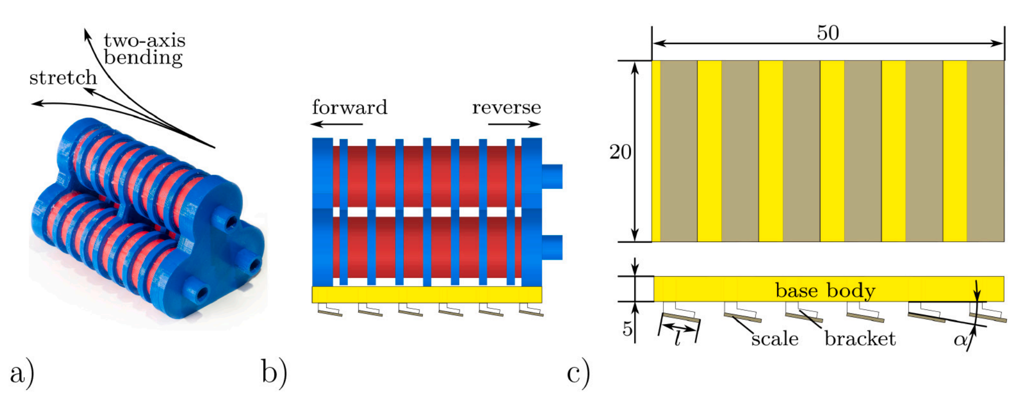

Fig. 1. a) Universal soft bending actuator [21] b) with artificial snakeskin attached, and c) dimensions of the artificial snakeskin (angle of attack α, length of the scales l).

different types of it with a wide range of stretchability. For the artificial snakeskin we used two silicons with different stiffness to investigate which stiffness leads to a higher friction anisotropy. One silicone is a soft *Ecoflex® 00–50* (*Smooth-On Inc., USA*), which has a hardness of 50 (Shore 00) and allows stretching up to 980%. Note that *Ecoflex® 00–50*, although soft, is the stiffest silicone of the *Ecoflex®*-Series. The other silicone used is a relatively stiff *ADDV-42* (*R&G Verbundwerkstoffe GmbH, Germany*), having a hardness of 40 (Shore A) and allowing stretching up to 400%.

2.2.2. Brackets

The brackets define the angle of attack of the scales (10 deg., 20 deg., and 30 deg. in this study) and connect the same with the base body without lowering its stretching capability. They are cast in the base body material and form a unit with it. Comparable to the roots of a tree anchoring it to the ground, the embedded part of the bracket needs to give stability and a tight connection to the base material.

The brackets are manufactured by 3D-printing. For our application, there is no difference whether to use polylactic acid (PLA) or acrylonitrile butadiene styrene (ABS) filament. Both materials are stiff enough to prevent the bracket from bending. Consequently, the base body material is the only parameter to tune the stiffness of mounting.

2.2.3. Scales

The scales are in permanent contact to the ground and must be resistant to wear, which is achieved by a 0.3 mm glass fiber resin plate (*Carbotec, Germany*). Due to the composite material, the scales are robust and stiff (flexural strength 18.000 MPa), but easy to work with. Furthermore, their surface is smooth and even and therefore beneficial for gluing them on the brackets. The edges of the scales should be pretreated with abrasive paper to ensure similar initial conditions.

The length of the scales is variable to the users needs. For our investigation, we use a length of 6 mm, Fig. 1c. This causes the scales to overlap the bracket by 1 mm.

2.3. Manufacturing Process

The central element of the manufacturing process of the artificial skin is a mold for the base body, as shown in Fig. 2. The mold consists of two parts in order to facilitate the demolding process: a lower base part and the wall.

To keep the brackets in position during the molding process, they are connected to each other by a support structure and printed as a single part. The brackets with support structure are fixed on the mold and the silicone is poured in. After curing and demolding, the silicone keeps the brackets in position and the support structure can be cut off.

The scales are cut either by scissors or by a cutting machine. Adhesive tape is used to attach the scales to the brackets. In order to achieve a strong connection of the brackets and the scales, the brackets need to be cleaned from remaining silicone by a solvent.

2.4. Expectations

Real snakes move their scales in order to adapt friction to the current situation [7]. When varying the angle of attack, we expect a higher friction coefficient both in forward and in reverse direction at larger angles. Consequently, we expect to find an intermediate angle of attack at which the friction anisotropy is higher than for the others, due to a compromise between low forward and high reverse friction.

The angle of attack is actively adapted by real snakes, but only passively by the elastic forces of the base body material, like in the model in [5]. Knowing from the model that an “intermediate stiffness” provides the highest friction anisotropy, we chose two silicons with different stiffness for the base body material. We expect that the softer silicone is closer to an intermediate stiffness in our case and reduces the friction coefficient in forward direction because the scales are able to bend upwards, while it increases the friction coefficient in reverse direction because the scales are able to interlock with the roughness of the ground.

3. Experimental Setup

In our experimental study, we were interested to identify the effects of the stiffness of the base body material and of the angle of attack on the friction coefficient in forward and reverse direction separately. For this purpose, several prototypes of artificial snakeskin were tested on a linear friction test bench without being mounted on a soft actuator, in order to reduce influences of surrounding factors.

3.1. Test Bench

Referring to Fig. 3a, the test bench is based on a linear guiding with a denim textile mounted on its movable table while the prototype is fixed into position. The denim textile is related to a work of [4] in which the

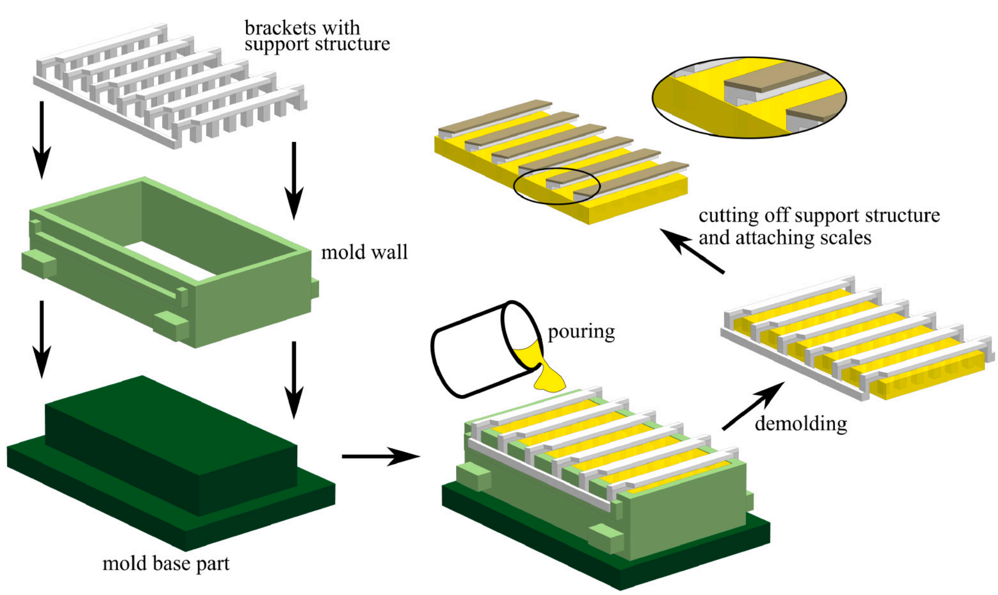

Fig. 2. Manufacturing process of the artificial snakeskin.

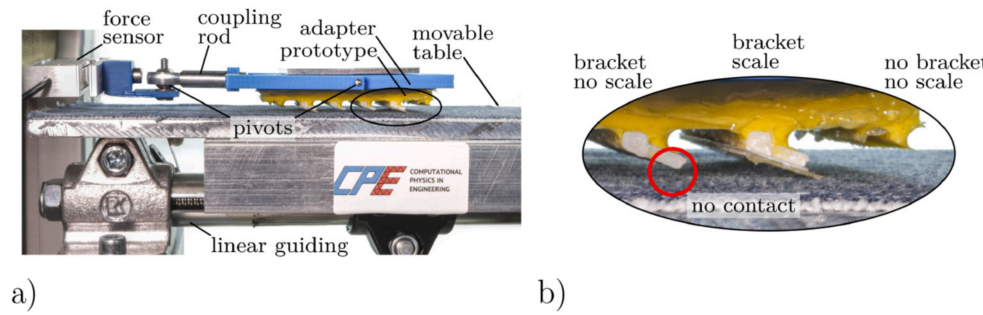

Fig. 3. a) Test bench and b) prototype adapted for testing.

authors determine the friction coefficients of milk snakes on textile. In the perspective of Fig. 3a, the table of the linear guiding moves to the right during testing. The pulling speed of the linear guiding was set to 5 mm/s for all experiments.

The prototypes are glued to an adapter with *Sil-Poxy* silicone glue (*Smooth-On Inc., USA*) without being stretched. The adapter plate has an embedded groove matching to the size of the prototypes, which increases the reproducibility of mounting. By attaching a weight at the top of the adapter plate, the weight of a soft actuator, on which the snakeskin will be attached in an application, can be simulated. In our case, the weight of holder and deadweight were approximately 30 g.

A *KD-42 s 1 N (ME-Meßsysteme, Germany)* force sensor measures the horizontal tensile forces of the prototype when the table of the linear guiding moves. The adapter plate with the prototype is attached to the force sensor by a coupling rod and two pivots. The pivots are important to ensure that the prototype lies flat on the surface without any interfering normal forces due to the coupling with the force sensor.

Each experiment was recorded for a subsequent video analysis. We used a *Canon EOS 750D* reflex camera.

3.2. Prototypes

For the study, we tested prototypes with two different base body silicons (*Ecoflex® 00–50* and *ADDV-42*) and brackets with three angles of attack (10 deg., 20 deg., 30 deg). To reduce the influence of hand manufacturing on the results, we manufactured two prototypes for each parameter configuration (silicone/angle), which makes twelve prototypes in total.

Due to a clear identification of the prototypes, the denotation in the following is always *silicone-angle-number*, for example *Ecoflex-10-1* or *ADDV-20-2*. The last attribute (*number*) can be *1* or *2* in order to distinguish between two prototypes of the same silicone and angle. To specify several prototypes with a combining attribute, the varying attributes are indicated as *X*. For example, the specification of all prototypes with an angle of 20 deg. is *X-20-X*.

For testing, we removed the outermost brackets and scales as well as the innermost scales of the prototypes, as can be seen in Fig. 3b. We removed the former since the fringe areas of the base body are softer, and the softness might differ between prototypes. For the latter, we only removed the scales in order to prevent cavities in the base body that might change its behavior. In none of the experiments did the brackets touch the ground. With only two remaining scales we can ensure a continuous and uniform contact between the artificial snakeskin and the ground with reduced interfering effects, such as mutually influencing scales, edge effects or inaccuracies of the hand manufacturing.

3.3. Test Procedure

To measure the friction force and to calculate the friction coefficient, three measurements with each prototype were performed in forward and reverse direction. Each of the measurements consists of nine periods of 3 s each of pulling the surface under the prototype and pausing, cf. Fig. 4. Compared to a continuous pulling, pulling and pausing allows to identify possible dynamic run-in effects. In fact, such effects did not appear in our measurements, but the measurements are not disturbed by the pausing periods.

We checked the distribution of the measured values of each pulling period for peculiarities, and determined its mean friction coefficient. Hereby, we assumed a static normal load corresponding to the weight of the respective prototype plus adapter. For the analysis, the first pulling period was neglected in order to suppress errors, which might be caused by a rearrangement of the prototypes during the first movement. Consequently, we gain eight friction coefficients per measurement, which will be called “block-mean values” in the following.

With three measurements for each prototype and direction, twelve prototypes, eight block-mean values per measurement, and four invalid measurements (32 block-mean values) at which the prototype did not follow a straight track, the data set consists of 544 block-mean values to be analyzed. Statements, whether a grouping parameter (e.g. the angle of attack or the number of measurement) has a statistical influence on the friction coefficient or not, are based on a Kruskal–Wallis one-way ANOVA ($p < 0.001$) of the block-mean values, followed by a pairwise multiple comparison procedure (Dunn’s Method, $p < 0.05$). In rare cases with only two groups, and a normality test and an equal variance test passed, they are based on a standard one-way ANOVA ($p < 0.001$), followed by a pairwise comparison procedure (Holm-Sidak method, $p < 0.05$).

4. Results

The distribution of the block-mean values, categorized by prototypes and direction, are shown in Fig. 5 (*Ecoflex-X-X*) and in Fig. 6 (*ADDV-X-X*). As intended in the design of the artificial snakeskin, each of the prototypes has a statistically significant friction anisotropy in forward-reverse direction.

First, we start with a video analysis of the experiments, and we discuss influences of the measurement order and of the hand manufacturing on the measurements. We then turn to the subject of this study by discussing the influence of the base body material and of the angle of attack on the friction coefficient. For each subsection, detailed information on the basic populations and the grouping parameters of the

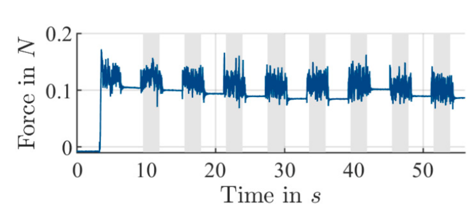

Fig. 4. Example for the recorded friction force over time for one measurement. Gray areas indicate the periods of pulling that were considered for the data analysis.

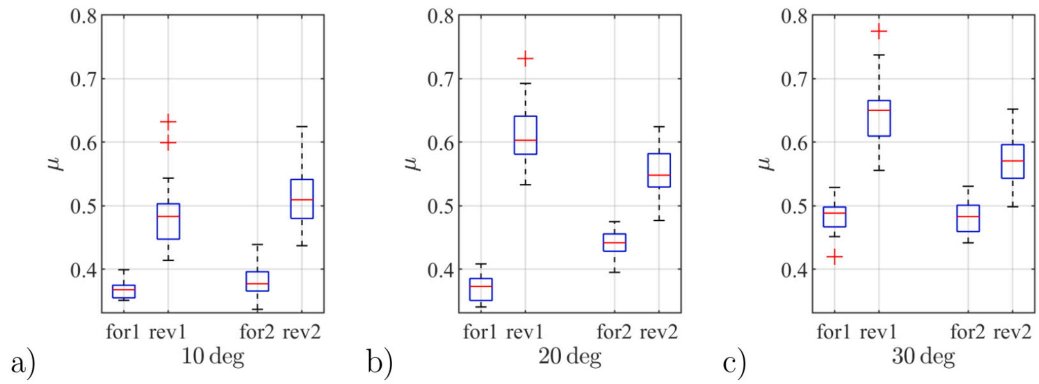

Fig. 5. Distribution (median, quantils, total range and outliers) of the block-mean values for the *Ecoflex-X-X* prototypes and different angles. For each of the three angles, two prototypes were tested in both forward and reverse direction.

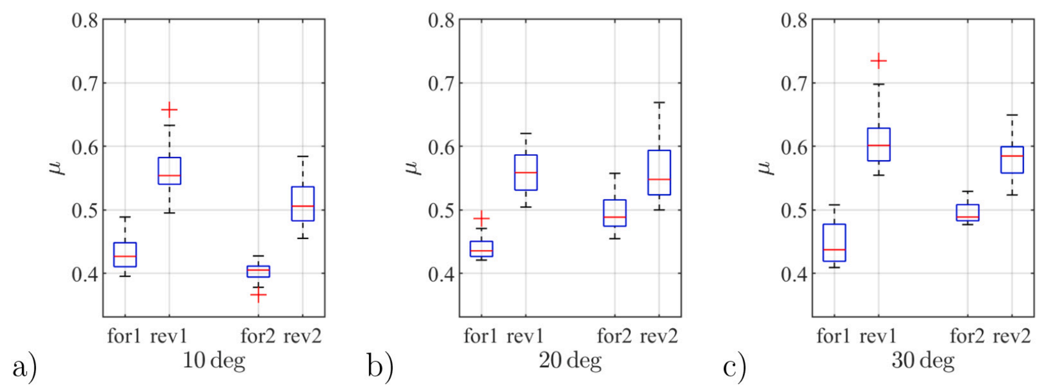

Fig. 6. Distribution of the block-mean values (median, quantils, total range and outliers) for the *ADDV-X-X* prototypes and different angles. For each of the three angles, two prototypes were tested in both forward and reverse direction.

underlying tests can be found in the Appendix.

4.1. Video Analysis

In general, the prototypes run much smoother in forward direction than in reverse direction. This is in accordance to the variance of the measured friction forces in Figs. 5 and 6, which is larger for measurements in reverse direction.

As will be shown in the following, the *ADDV-X-X* prototypes differ significantly between counterparts of the same silicone and angle, see Subsection 4.3, and between different angles of attack, see Subsection 4.5. However, in the videos no differences of the dynamic behavior and no individual motion of the scales are visible (Supplementary Videos S1 and S2).

In contrast, some of the *Ecoflex-X-X* prototypes' scales clearly show a little motion during the experiments, although a reliable quantification was not possible with the equipment used. Interestingly, prototypes showing a larger motion of the scales (*Ecoflex-10-2, Ecoflex-20-1* and *Ecoflex-30-1*) tend to provide higher reverse friction (Fig. 5) than their counterpart of the same silicone and angle due to interlocking with the ground (Fig. 7a).

One of the scales of prototype *Ecoflex-20-1* is accidentally mounted more flexible than the scales of the other prototypes and was able not only to interlock with the ground in reverse direction but also to bend upwards in forward direction (Fig. 7b and Supplementary Videos S3 and S4). As can be seen in Fig. 5b, this causes a significantly lower friction coefficient in forward direction than that of its counterpart *Ecoflex-20-2* (Supplementary Videos S5 and S6), and is evidence for the working principle of our novel design: achieving friction anisotropy with a flexible base body material. Because there are no significant, visible differences between the counterpart prototypes *Ecoflex-20-X*, a probable explanation of this result is an insufficient gluing of the prototype *Ecoflex-20-1* to the adapter plate at the position of the responsible scale.

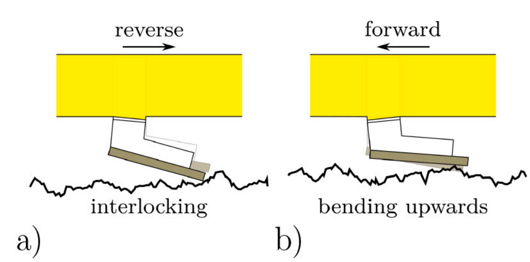

Fig. 7. Scheme of the scales' movement observed in the video analysis.

4.2. Influence of Measurement Order

Each of the prototypes is measured three times for each direction. Each measurement consists of eight periods of pulling (block-mean values), dividing the test track in sections. The test data show that the position of the prototype on the test track has no significant influence on the friction coefficient. However, although there should be no difference in friction coefficient between measurements with the same prototype, the friction coefficient decreases statistically significant from one measurement to the other for seven prototypes. For five prototypes the test data do not allow to exclude the possibility of the same.

The reason for the decreasing friction coefficient is a changing behavior of the scales over time. The scales of all prototypes are pretreated by the use on abrasive paper to smoothen the lower edges of the scales after cutting. However, in remaining rough areas, microscopic fibers of the denim textile become entangled over time which reduces the friction coefficient. In contrast, wear of the denim textile is not a proper explanation because the effect is the same for all prototypes, independent of whether they were tested at first on the new denim or at last on the used denim. Furthermore, any kind of fatigue or softening effects of the base body material are not a proper explanation as well, because all prototypes show the same change of the friction coefficient, although there is visibly more motion of the scales of the *Ecoflex-X-X* prototypes than of the *ADDV-X-X* prototypes.

Since the decrease of friction is the same for all prototypes, this effect is not relevant for conclusions on the base body material and the angle of attack of the scales. Rather, it emphasizes the necessity to take the contacting edges of the scales, which were neglected for this investigation (subsection 2.1), into account in future work.

Some of the distributions in Figs. 5 and 6 contain outliers. Their occurrence cannot be associated with the measuring order. For the reverse outliers, the most probable explanation is an unusual interlocking of the scale with the denim textile. For the forward outliers, an unusual bending upwards for single pulling periods due to dynamic run-in effects is the most probable explanation.

4.3. Influence of Hand Manufacturing

Hand manufacturing of prototypes is critical to the reproducibility of experiments. To counteract this, for each combination of base body material and angle of attack, two prototypes were manufactured. Ideally, there should be no differences between two prototypes of the same configuration.

However, the *ADDV-X-X* prototypes in Fig. 6 differ in their behavior. Although there is no visible difference of the dynamic behavior in the video analysis of the experiments, each of the prototype pairs differs significantly in both directions (except *ADDV-20-X* in reverse direction). Scales that are imprecisely taped to the bracket and whose lower edges are therefore not parallel to the ground might be a source of error.

In contrast, the counterpart prototypes *Ecoflex-10-X* and *Ecoflex-30-X* in Fig. 5a/c both behave similar to each other. This implies that the soft body material more efficiently compensates inaccuracies of the hand manufacturing, which is an important finding to manufacture artificial snakeskin with reproducible properties in future work. Only the *Ecoflex-20-X* prototypes in Fig. 5b significantly differ from each other in forward as well as in reverse direction, which is due to the flexible fixation of the prototype *Ecoflex-20-1*, as explained in the video analysis Subsection 4.1.

4.4. Influence of Base Body Material

In Subsection 2.4, we provided the hypothesis that the softer silicone *Ecoflex® 00–50* has the higher friction anisotropy. Comparing all prototypes among each other, the forward friction coefficient supports this hypothesis because it is significantly lower for the *Ecoflex-X-X* prototypes than for the *ADDV-X-X* prototypes. In reverse direction, the test data do not allow a clear distinction between the silicons. However, the measurements indicate that the difference between both silicons is at least lower in the reverse direction than in the forward direction.

A more differentiated view can be achieved by comparing the different angles separately, for example *Ecoflex-10-X* against *ADDV-10-X*. While there is a significant difference between both materials for the *X-10-X* and *X-20-X* prototypes, there is none for the *X-30-X* prototypes. Interestingly, the friction coefficient of the *Ecoflex-10-X* prototypes is lower in both directions than of the *ADDV-10-X* prototypes, see Figs. 5/6a. Referring to the expectations in Subsection 2.4, the friction coefficient in reverse direction should be higher, which leads us to the assumption that the scales are not able to interlock in reverse direction because the base body material does not allow enough flexibility, although *Ecoflex® 00–50* is the softer material in this study.

For the *X-20-X* prototypes in Figs. 5/6b, the analysis is more complex. Taking all four *X-20-X* prototypes into account, there is a significant difference between the materials, with the friction coefficient of the softer material being lower in forward and being higher in reverse direction. However, prototype *Ecoflex-20-1* provides an exceptionally high friction anisotropy, as already mentioned in Subsection 4.1. Considering only the prototype *Ecoflex-20-2*, the forward friction of the same is still significantly lower than that of the *ADDV-20-X* prototypes. In reverse direction, the median of the *Ecoflex-20-2* block-mean values is lower than the median of the *ADDV-20-X* prototypes, which is similar to the frictional properties of the *X-10-X* prototypes.

This implies that the flexibility of the base body material is highly important for the motion of the scales and their interlocking with the ground. Since only the prototype *Ecoflex-20-1* meets the expectations in Subsection 2.4 to full extent, also the fixation of the artificial snakeskin to the soft robot must be considered. Nevertheless, if the snakeskin shall be attached over the entire area of the base body, *Ecoflex® 00–50*, as the softer silicone used in this study, seems still not flexible enough to achieve an optimal skin behavior.

4.5. Influence of Angle of Attack

Besides the base body material, the angle of attack is the second parameter to be investigated in this study. In Subsection 2.4 we provided the hypothesis that forward and reverse friction coefficients both increase with a larger angle of attack. Indeed, the test data support this hypothesis for the *Ecoflex-X-X* prototypes (Fig. 5) and the *ADDV-X-X* prototypes (Fig. 6) each compared among themselves. The measurements show only two exceptions where no significant differences appear: *Ecoflex-20-X* against *Ecoflex-30-X* in reverse direction and *ADDV-20-X* against *ADDV-30-X* in forward direction. This is an indication that the effects of the angle of attack decrease as the angles become larger.

More relevant than the absolute friction coefficients is the friction anisotropy provided by the prototypes. It can be quantified as the ratio of reverse and forward friction μ_r/μ_f, as compared in Table 1. The coefficients of friction μ_r and μ_f are determined as the median of all block-mean values of one prototype. While the absolute coefficient of friction depends on the angle of attack in either direction, there is no clear dependency on the friction ratios.

However, the novel design approach is still promising as the friction ratio of several prototypes is close to the friction ratio of 1.4 observed for milk snakes [4]. Prototype *Ecoflex-20-1* has an even higher friction ratio of 1.6. This is because this prototype meets the expectations for flexible mounting to a particularly high degree, as shown in the video analysis Subsection 4.1. Since only the scales of this prototype move to a high extent, no optimized angle of attack can be derived for the selected silicons.

Table 1
Friction ratios μ_r/μ_f of the twelve prototypes.

Material	Angle	No.	μ_r/μ_f
Ecoflex	*10*	*1*	1.31
		2	1.35
	20	*1*	1.62
		2	1.24
	30	*1*	1.33
		2	1.18
ADDV	*10*	*1*	1.30
		2	1.25
	20	*1*	1.28
		2	1.12
	30	*1*	1.38
		2	1.20

5. Conclusions

In this work, we present a novel design of an artificial snakeskin for soft robotics. Due to its modularity, it is beneficial for a systematic analysis of friction properties and for easy customizing of the components depending on the current needs. The artificial snakeskin consists of a flexible base with brackets embedded which define the angle of attack and on which scales are fixed. The flexible base body material allows a limited motion of the scales and thereby increases the friction anisotropy of the artificial skin. We used two silicons and three angles of attack to investigate their influence on the frictional properties of our artificial snakeskin. Investigations on the microstructure of the scales and the shape of the scales' edges are left to future work.

All manufactured prototypes provide a statistically significant friction anisotropy in forward-reverse direction. Hereby, the friction ratio of several prototypes is close to that of a milk snake, while prototype *Ecoflex-20-1* provides even a higher friction anisotropy. The reason is an exceptionally high flexibility of one of its scales. It can be concluded that a softer base body material would be of advantage to increase the friction anisotropy of our prototypes in general. Whether a base body, which is too soft, lowers friction anisotropy needs to be clarified.

Apart from that, the investigation provides important general information. A soft base body material is beneficial in order to reduce the influence of hand manufacturing, independent of whether a passive motion of the scales is desired or not. Furthermore, the shape of the scales' edges is not only a design parameter to increase friction anisotropy but also it provides the opportunity to reduce run-in effects and to achieve a stable frictional behavior.

These findings are a promising piece of groundwork for adapting the parameters of our artificial snakeskin to a snake-like robot of choice in future. Thereby, it must be taken into account that the stiffness of mounting is rather depending on the leverage than just only on the base body material. Hence, to tune the artificial skin to a desired stiffness, the weight of the actuator and the length of the scales must additionally be taken into account. Another less obvious possibility to change the motion of scales is to adjust the embedded part of the bracket.

The Supplementary Videos S7 and S8 present an actuator which crawls by help of our artificial snakeskin. Considering the findings regarding the base body material, the artificial snakeskin is made of *Ecoflex® 00–30*, which is softer than *Ecoflex® 00–50*. The fiber angle is 20 deg.

Our current approach of an artificial snakeskin imitates the scales of the belly of a snake and therefore only provides friction anisotropy in forward-reverse direction, which limits the robot to a rectilinear gait. Consequently, an improved artificial snakeskin that also has a high transverse friction coefficient would be a great benefit in future. The simplest method to achieve this is to divide the scales into halves and turn them in opposite direction such that the direction of highest friction of the snake-like robot changes from reverse direction to transverse direction. A more promising, but more complex method is to add additional small scales with altered properties for transverse motion at both sides of the robot's belly, similar to real snakes.

Supplementary data to this article can be found online at https://doi.org/10.1016/j.biotri.2022.100210.

Declaration of Competing Interest

None.

Acknowledgement

Funded by the Deutsche Forschungsgemeinschaft (DFG, German Research Foundation) – 404986830 – SPP2100.

Appendix

In the following, we present the basic population and the treatment groups which lead to the explications in the results Section 4.

General finding, introduction ofSection 4

basic population	grouping parameter
Each prototype seperately	direction

Measurement order,Subsection 4.2

basic population	grouping parameter
Each prototype seperately	block-mean value number
Each prototype seperately	measurement

Hand manufacturing,Subsection 4.3

basic population	grouping parameter
Ecoflex-10-X, forw.	number
Ecoflex-10-X, rev.	number
Ecoflex-20-X, forw.	number
Ecoflex-20-X, rev.	number
Ecoflex-30-X, forw.	number
Ecoflex-30-X, rev.	number
ADDV-10-X, forw.	number
ADDV-10-X, rev.	number
ADDV-20-X, forw.	number
ADDV-20-X, rev.	number
ADDV-30-X, forw.	number
ADDV-30-X, rev.	number

Base body material, subection 4.4

basic population	grouping parameter
X-X-X, forw.	material
X-X-X, rev.	material
X-10-X, forw.	material
X-10-X, rev.	material
X-20-X, forw.	material
X-20-X, rev.	material
X-30-X, forw.	material
X-30-X, rev.	material
Ecoflex-20-2 + *ADDV-20-X*, forw.	material
Ecoflex-20-2 + *ADDV-20-X*, rev.	material

Angle of attack,Subsection 4.5

basic population	grouping parameter
Ecoflex-X-X, forw.	angle
Ecoflex-X-X, rev.	angle
ADDV-X-X, forw.	angle
ADDV-X-X, rev.	angle

References

[1] H.A. Abdel-Aal, Surface structure and tribology of legless squamate reptiles, J. Mech. Behav. Biomed. Mater. 79 (2018) 354–398, https://doi.org/10.1016/j.jmbbm.2017.11.008.

[2] S. Hirose, H. Yamada, Snake-like robots, IEEE Robot. Automat. Mag. 16 (1) (2009) 88–98, https://doi.org/10.1109/MRA.2009.932130.

[3] A.E. Filippov, S.N. Gorb, Modelling of the frictional behaviour of the snake skin covered by anisotropic surface nanostructures, Sci. Rep. 6 (1) (2016), https://doi.org/10.1038/srep23539.

[4] D.L. Hu, J. Nirody, T. Scott, M.J. Shelley, The mechanics of slithering locomotion, Proc. Natl. Acad. Sci. 106 (25) (2009) 10081–10085, https://doi.org/10.1073/pnas.0812533106.

[5] A. Filippov, S.N. Gorb, Frictional-anisotropy-based systems in biology: structural diversity and numerical model, Sci. Rep. 3 (1) (2013), https://doi.org/10.1038/srep01240.

[6] M.J. Baum, A.E. Kovalev, J. Michels, S.N. Gorb, Anisotropic friction of the ventral scales in the snake lampropeltis getula californiae, Tribol. Lett. 54 (2) (2014) 139–150, https://doi.org/10.1007/s11249-014-0319-y.

[7] H. Marvi, J.P. Cook, J.L. Streator, D.L. Hu, Snakes move their scales to increase friction, Biotribology 5 (2016) 52–60, https://doi.org/10.1016/j.biotri.2015.11.001.

[8] C. Tiner, S. Bapat, S.D. Nath, S.V. Atre, A. Malshe, Exploring convergence of snake-skin-inspired texture designs and additive manufacturing for mechanical traction, Procedia Manuf. 34 (2019) 640–646, https://doi.org/10.1016/j.promfg.2019.06.116.

[9] J.K. Hopkins, B.W. Spranklin, S.K. Gupta, A survey of snake-inspired robot designs, Bioinspiration & Biomimetics 4 (2) (2009), 021001.

[10] K.Y. Pettersen, Snake robots, Annu. Rev. Control. 44 (2017) 19–44, https://doi.org/10.1016/j.arcontrol.2017.09.006.

[11] R. Khan, M.M. Billah, N.M.L. Huq, M. Helmi, S.M. Ahmmed, Investigation on data extraction trends for snake robot, Procedia Comput. Sci. 42 (2014) 145–152, https://doi.org/10.1016/j.procs.2014.11.045.

[12] H. Marvi, G. Meyers, G. Russell, D.L. Hu, Scalybot: A Snake-Inspired Robot with Active Control of Friction, 2011, https://doi.org/10.1115/DSCC2011-6174.

[13] M.M. Serrano, A.H. Chang, G. Zhang, P.A. Vela, Incorporating Frictional Anisotropy in the Design of a Robotic Snake Through the Exploitation of Scales, 2015, https://doi.org/10.1109/ICRA.2015.7139717.

[14] M. Luo, M. Agheli, C.D. Onal, Theoretical modeling and experimental analysis of a pressure-operated soft robotic snake, Soft Robot. 1 (2) (2014) 136–146, https://doi.org/10.1089/soro.2013.0011.

[15] P. Boyraz, G. Runge, A. Raatz, An overview of novel actuators for soft robotics, Actuators 7 (3) (2018), https://doi.org/10.3390/act7030048. URL, http://www.mdpi.com/2076-0825/7/3/48.

[16] Y. Cao, Y. Liu, Y. Chen, L. Zhu, Y. Yan, X. Chen, A novel slithering locomotion mechanism for a snake-like soft robot, J. Mech. Phys. Solid 99 (2017) 304–320, https://doi.org/10.1016/j.jmps.2016.11.019.

[17] A. Rafsanjani, Y. Zhang, B. Liu, S.M. Rubinstein, K. Bertoldi, Kirigami skins make a simple soft actuator crawl, Sci. Robot. 3 (15) (2018) eaar7555, https://doi.org/10.1126/scirobotics.aar7555.

[18] T.D. Ta, T. Umedachi, Y. Kawahara, Design of Frictional 2d-Anisotropy Surface for Wriggle Locomotion of Printable Soft-Bodied Robots, 2018, https://doi.org/10.1109/ICRA.2018.8463177.

[19] B. Liu, Y. Ozkan-Aydin, D.I. Goldman, F.L. Hammond, Kirigami skin improves soft earthworm robot anchoring and locomotion under cohesive soil, in: 2019 2nd IEEE International Conference on Soft Robotics (RoboSoft), IEEE, 2019, https://doi.org/10.1109/robosoft.2019.8722821.

[20] C. Branyan, R.L. Hatton, Y. Menguc, Snake-inspired kirigami skin for lateral undulation of a soft snake robot, IEEE Robot. Automat. Lett. 5 (2) (2020) 1728–1733, https://doi.org/10.1109/lra.2020.2969949.

[21] F. Lamping, K.M. de Payrebrune, A systematically derived design for a modular pneumatic soft bending actuator, in: 2022 5th IEEE International Conference on Soft Robotics (RoboSoft), IEEE, 2022 in press.

[22] An anisotropic imitation scales bellows structure and preparation method of friction, (China Patent No. 104723346B) (2016).